Self-consistent optical constants of MgF$_2$, LaF$_3$, and CeF$_3$ films

LUIS V. RODRÍGUEZ-DE MARCOS,[1,2] JUAN I. LARRUQUERT,[1,*] JOSÉ A. MÉNDEZ,[1] AND JOSÉ A. AZNÁREZ[1]

[1]*GOLD-IO-CSIC Instituto de Óptica-Consejo Superior de Investigaciones Científicas, Serrano 144, 28006 Madrid, Spain*
[2]*lv.rodriguez@io.cfmac.csic.es*
*j.larruquert@csic.es

Abstract: Various fluorides are materials in nature that extend their transparency range to the shortest wavelengths in the far ultraviolet (FUV, 100nm<λ<200 nm). These are relevant materials to prepare multilayer coatings in the FUV for demanding applications such as space instrumentation for astrophysics, solar physics and atmosphere physics, as well as free electron lasers, plasma diagnostics, synchrotron radiation, lithography, spectroscopy, etc. Multilayer design requires the optical constants of the coating materials. Multilayers optimally alternate two transparent materials with contrasting refractive indices. The optical constants of a low-index material, MgF$_2$, and of two high-index materials, LaF$_3$ and CeF$_3$, have been determined in a wide spectral range and are presented here. Thin films of MgF$_2$, LaF$_3$, and CeF$_3$ were deposited by boat evaporation onto substrates at 523 K. Transmittance, reflectance, and ellipsometry measurements were performed in ranges jointly covering the 30-950-nm spectral range. This range was extended with literature data and extrapolations to obtain self-consistent optical constants using the Kramers-Kronig (KK) analysis. An iterative, double KK analysis procedure (successive reflectance-phase and *k-n* KK analyses) was carried out to obtain a self-consistent set of optical constants per material. With the final data sets, the experimental measurements were satisfactorily reproduced. Global self-consistency of the data sets was successfully evaluated through sum rules; additionally, local self-consistency at each photon energy range was also evaluated through a novel sum-rule method which involves window functions. The new sets of optical constant extend the data availability mainly to the FUV and beyond, particularly for CeF$_3$, where few data had been reported.

References and links

1. M. Zukic, D. G. Torr, J. Kim, J. F. Spann, and M. A. Torr, "Filters for the International Solar Terrestrial Physics Mission far-ultraviolet imager," Opt. Eng. **32**(12), 3069–3074 (1993).
2. S. Günster, D. Ristau, A. Gatto, N. Kaiser, M. Trovó, and M. Danailov, "Storage ring free-electron lasing at 176 nm--dielectric mirror development for vacuum ultraviolet free-electron lasers," Appl. Opt. **45**(23), 5866–5870 (2006).
3. D. Ristau, S. Günster, S. Bosch, A. Duparré, E. Masetti, J. Ferré-Borrull, G. Kiriakidis, F. Peiró, E. Quesnel, and A. Tikhonravov, "Ultraviolet optical and microstructural properties of MgF$_2$ and LaF$_3$ coatings deposited by ion-beam sputtering and boat and electron-beam evaporation," Appl. Opt. **41**(16), 3196–3204 (2002).
4. R. Thielsch, "Optical coatings for the DUV/VUV," *Optical Interference Coatings*, N. Kaiser and H.-K. Pulker, eds., Vol. 88 of Springer Series in Optical Sciences (Springer, 2003), pp. 257–280.
5. L. J. Lingg, "Lanthanide trifluoride thin films: structure, composition, and optical properties," Thesis, Univ. Arizona, 1990.
6. M. Zukic, D. G. Torr, J. F. Spann, and M. R. Torr, "Vacuum ultraviolet thin films. 1: Optical constants of BaF$_2$, CaF$_2$, LaF$_3$, MgF$_2$, AlO$_3$, HfO$_2$, and SiO$_2$, thin films," Appl. Opt. **29**(28), 4284–4292 (1990).
7. C. Xue, K. Yi, C. Wei, J. Shao, and Z. Fan, "Determination of optical constants in the VUV range for fluoride thin films," Proc. SPIE **7283**, 72831E (2009).
8. S. Shuzhen, S. Jianda, L. Chunyan, Y. Kui, F. Zhengxiu, and C. Lei, "High-reflectance 193 nm Al$_2$O$_3$/ MgF$_2$ mirrors," Appl. Surf. Sci. **249**(1-4), 157–161 (2005).

9. A. V. Tikhonravov, M. K. Trubetskov, A. V. Krasilnikova, E. Masetti, A. Duparré, E. Quesnel, and D. Ristau, "Investigation of the surface micro-roughness of fluoride films by spectroscopic ellipsometry," Thin Solid Films **397**(1-2), 229–237 (2001).

10. D. Smith and P. Baumeister, "Refractive index of some oxide and fluoride coating materials," Appl. Opt. **18**(1), 111–115 (1979).

11. A. S. Barrière and A. Lachter, "Optical transitions in disordered thin films of the ionic compounds MgF_2 and AlF_3 as a function of their conditions of preparation," Appl. Opt. **16**(11), 2865–2871 (1977).

12. O. R. Wood II, H. G. Craighead, J. E. Sweeney, and P. J. Maloney, "Vacuum ultraviolet loss in magnesium fluoride films," Appl. Opt. **23**(20), 3644–3649 (1984).

13. J. Kolbe, H. Kessler, T. Hofmann, F. Meyer, H. Schink, and D. Ristau, "Optical properties and damage thresholds of dielectric UV/VUV-coatings deposited by conventional evaporation, IAD and lBS," Proc. SPIE **1624**, 221–235 (1992).

14. A. P. Lukirskii, E. P. Savinov, O. A. Ershov, and Yu. F. Shepelev, "Reflection coefficients of radiation in the wavelength range from 23.6 to 113 Å for a number of elements and substances and the determination of the refractive index and absorption coefficient," Opt. Spectrosc. **16**, 168–172 (1964).

15. W. F. Hanson, E. T. Arakawa, and M. W. Williams, "Optical properties of MgO and MgF_2 in the extreme ultraviolet region," J. Appl. Phys. **43**(4), 1661–1665 (1972).

16. T. T. Cole and F. Oppenheimer, "Polarization by reflection and some optical constants in the extreme ultraviolet," Appl. Opt. **1**(6), 709–710 (1962).

17. M. W. Williams, R. A. Macrae, and E. T. Arakawa, "Optical Properties of Magnesium Fluoride in the Vacuum Ultraviolet," J. Appl. Phys. **38**(4), 1701–1705 (1967).

18. F. Bridou, M. Cuniot-Ponsard, J.-M. Desvignes, M. Richter, U. Kroth, and A. Gottwald, "Experimental determination of optical constants of MgF_2 and AlF_3 thin films in the vacuum ultra-violet wavelength region (60–124 nm), and its application to optical designs," Opt. Commun. **283**(7), 1351–1358 (2010).

19. H. Venghaus, "Energieverlustmessungen und Bestimmungoptischer Konstanten von MgO und MgF_2," Opt. Commun. **2**(9), 447–451 (1971).

20. P. J. Martin, W. G. Sainty, R. P. Netterfield, D. R. McKenzie, D. J. H. Cockayne, S. H. Sie, O. R. Wood, and H. G. Craighead, "Influence of ion assistance on the optical properties of MgF_2," Appl. Opt. **26**(7), 1235–1239 (1987).

21. J. D. Targove, M. J. Messerly, J. P. Lehan, C. C. Weng, R. H. Potoff, H. A. Macleod, L. C. McIntyre, Jr., and J. A. Leavitt, "Ion-assisted deposition of fluorides," Proc. SPIE **678**, 115–122 (1986).

22. St. Günster, B. Görtz, D. Ristau, E. Quesnel, G. Ravel, M. Trovó, and M. Danailov, "IBS deposition of dense fluoride coatings for the vacuum ultraviolet free electron laser," Proc. SPIE **5963**, 59630I (2005).

23. H. Uhlig, R. Thielsch, J. Heber, and N. Kaiser, "Lanthanide tri-fluorides: a survey of the optical, mechanical and structural properties of thin films with emphasis of their use in the DUV – VUV- spectral range," Proc. SPIE **5963**, 59630N (2005).

24. R. Thielsch, J. Heber, S. Jakobs, N. Kaiser, and A. Duparré, "Optical, structural and mechanical properties of lanthanide trifluoride thin film materials for use in the DUV-spectral region," *Optical Interference Coatings*, Vol. 9 of OSA 1998 Technical Digest Series (Optical Society of America, Washington, D.C., 1998), pp. 116–118.

25. G. Hass, J. B. Ramsey, and R. Thun, "Optical properties of various evaporated rare earth oxides and fluorides," J. Opt. Soc. Am. **49**(2), 116–120 (1959).

26. P. Chindaudom and K. Vedam, "Determination of the optical constants of an inhomogeneous transparent LaF_3 thin film on a transparent substrate by spectroscopic ellipsometry," Opt. Lett. **17**(7), 538–540 (1992).

27. H. Yu, Y. Shen, Y. Cui, H. Qi, J. D. Shao, and Z. X. Fan, "Characterization of LaF_3 coatings prepared at different temperatures and rates," Appl. Surf. Sci. **254**(6), 1783–1788 (2008).

28. G. Stephan, M. Nisar, and A. Roth, "Spectre électronique du fluorure de lanthane dans l'ultraviolet extrême," C. R. Acad. Sc. Paris, **274 B**, 807–810 (1972).

29. B. von Blanckenhagen, D. Tonova, and J. Ullmann, "Application of the Tauc-Lorentz formulation to the interband absorption of optical coating materials," Appl. Opt. **41**(16), 3137–3141 (2002).

30. C. Dujardin, C. Pedrini, N. Garnier, A. N. Belsky, K. Lebbou, J. M. Ko, and T. Fukuda, "Spectroscopic properties of CeF_3 and $LuF_3:Ce^{3+}$ thin films grown by molecular beam epitaxy," Opt. Mater. **16**(1-2), 69–76 (2001).

31. S. M. Saini, "The role of f-states in the electronic and optical properties of rare-earth trifluorides (RF3, R=Ce and Gd): a full potential study," J. Mater. Sci. **47**(21), 7665–7670 (2012).

32. M. Altarelli, D. L. Dexter, H. M. Nussenzveig, and D. Y. Smith, "Superconvergence and Sum Rules for the Optical Constants," Phys. Rev. B **6**(12), 4502–4509 (1972).

33. L. V. Rodríguez-de Marcos, J. A. Méndez, and J. I. Larruquert, "Tuning sum rules with window functions for optical constant evaluation," J. Opt. **18**(7), 075606 (2016).

34. http://henke.lbl.gov/optical_constants/.

35. L. V. Rodríguez-de Marcos, J. I. Larruquert, J. A. Méndez, and J. A. Aznárez, "Self-consistent optical constants of SiO_2 and Ta_2O_5 films," Opt. Mater. Express **6**(11), 3622–3637 (2016).

36. M. Bischoff, D. Gäbler, N. Kaiser, A. Chuvilin, U. Kaiser, and A. Tünnermann, "Optical and structural properties of LaF_3 thin films," Appl. Opt. **47**(13), C157–C161 (2008).

37. H. R. Philipp, "Influence of Oxide Layers on the Determination of the Optical Properties of Silicon," J. Appl. Phys. **43**(6), 2835–2839 (1972).
38. H. R. Philipp, "Optical properties of non-crystalline Si, SiO, SiO_x and SiO_2," J. Phys. Chem. Solids **32**(8), 1935–1945 (1971).
39. C. Pedrini, B. Moine, J. C. Gacon, and B. Jacquier, "One- and two-photon spectroscopy of Ce^{3+} ions in LaF_3-CeF_3 mixed crystals," J. Phys. Condens. Matter **4**(24), 5461–5470 (1992).
40. Downloaded from the following web of Physical Reference Data, Physics Laboratory at NIST: http://physics.nist.gov/PhysRefData/FFast/Text/cover.html
41. D. L. Windt, "IMD: Software for modeling the optical properties of multilayer films," Comput. Phys. **12**(4), 360–370 (1998), http://www.rxollc.com/idl/index.html.
42. M. Altarelli and D. Y. Smith, "Superconvergence and sum rules for the optical constants: physical meaning, comparison with experiment, and generalization," Phys. Rev. B **9**(4), 1290–1298 (1974).
43. E. Shiles, T. Sasaki, M. Inokuti, and D. Y. Smith, "Self-consistency and sum-rule tests in the Kramers-Kronig analysis of optical data: applications to aluminum," Phys. Rev. B **22**(4), 1612–1628 (1980).

Introduction

Fluorides are common materials in optical coatings. One attractive feature is their wide transparency range, that for various fluorides it extends down to wavelengths in the far ultraviolet (FUV, 100 nm$<\lambda<$200 nm). Hence fluorides are first-choice materials to prepare FUV multilayer coatings which are demanded for various applications, such as space instrumentation for astrophysics, solar physics and atmosphere physics [1], as well as free electron lasers [2], lithography [3], plasma diagnostics, synchrotron radiation, spectroscopy, etc. A review of coatings for the FUV, including fluorides, was reported by Thielsch [4].

In order to design optical coatings, optical constants of the constituent materials are necessary. Multilayer coatings typically alternate two transparent materials with contrasting refractive indices. This research investigates the optical constants of MgF_2, a material with a relatively small refractive index in the FUV, and of LaF_3 and CeF_3, two materials with a relatively high refractive index in the same range.

Evaporation is a suitable technique to deposit fluoride films that are transparent in the FUV. One advantage of fluorides over oxides or nitrides is that usually their molecules do not dissociate upon evaporation, so that films are easier to grow with a good stoichiometry, and reactive deposition is not required. The optical constants of thin films depend on film-growth conditions, such as substrate temperature, the presence of ion assistance, etc. In the transparency range of the materials, transparency is typically favoured by a higher substrate temperature during thin-film deposition; this is most important in the short FUV close to the material cutoff in order to make the extinction coefficient k small enough to prepare efficient multilayer coatings. In the transparency range, k of the fluoride can vary with substrate temperature during deposition over orders of magnitudes. Therefore, optical-constant data should be available for films deposited at a temperature close to the one to be used in the application. Measuring small values of k is not straightforward since no photometric or ellipsometric variable is made to significantly vary with small values of k. On the other hand, at wavelengths beyond the fluoride cutoff, the dependence of k on substrate temperature is expected to be less dramatic. In this research, fluoride films have been deposited by evaporation with thermal sources onto substrates heated at a temperature of 523 K.

Literature has reported several sets of FUV optical-constant data on MgF_2 and LaF_3. Regarding CeF_3, almost no FUV data was found for thin films. A thesis dissertation systematically investigated the optical properties of most lanthanide trifluorides [5]; unfortunately, LaF_3 and CeF_3 were not included in that research. Here a summary is presented of the literature providing optical constants of films deposited by evaporation on substrates at a temperature relatively close to the one used in this research. Such data have been often reported in narrow spectral ranges and it typically lacks self-consistency.

A considerable number of papers have been devoted to the optical constants of MgF_2 films deposited by evaporation. Literature provides data on the reflective index n in a wide range from close to the cutoff (~115 nm) up to the visible [2, 3, 6–9], and an extension up to 2000 nm with a Sellmeier model [10]. Regarding the extinction coefficient k or the absorption

coefficient α, there have been data reported between the cutoff up to ~600 nm [2, 6–8, 11]. Some papers report on optical constants of MgF_2 films deposited at considerably larger temperatures [4, 12, 13]. At wavelengths below MgF_2 cutoff, no data was found for films deposited in conditions similar to the present ones and most reported data are for films deposited at room temperature (sometimes temperature was not specified, which might be interpreted as that there was no substrate heating) [14–18]. Anyway, as mentioned above, the dependence of k and probably also n on substrate temperature is expected to be less dramatic at wavelengths shorter than the cutoff. Most papers involve optical measurements, but there are also optical constants obtained from electron energy-loss spectroscopy measurements [19]. Several reports on optical constants of MgF_2 deposited by other techniques can be also found in the literature [13, 20–22].

There is also a relatively large number of papers reporting optical constants of LaF_3. The following summary presents again the literature providing optical constants of LaF_3 films deposited by evaporation on substrates at a temperature relatively close to the one used in this research. As with MgF_2, there are several papers that provide n in a wide range from close to the cutoff (~120 nm) up to the infrared [2, 3, 6, 7, 23–25], some of them using a Sellmeier model [10, 26]. Regarding k, again most data are for wavelengths in the UV down to the cutoff [2, 6, 7, 23, 27]. There are also papers with optical constants of LaF_3 films deposited at much larger temperatures [4, 13]. At wavelengths below LaF_3 cutoff, only one paper was found, which reports a film deposited by evaporation on a nonheated substrate [28]. Several reports on optical constants of LaF_3 films deposited by other techniques can be also found in the literature [20, 22, 29].

In contrast, very limited data on optical constants of CeF_3 films were found in the literature. Hass et al. [25] obtained the optical constants of CeF_3 films grown with a substrate temperature of 573 K in the 220-2000-nm range. Smith and Baumeister obtained n in the 250-2000-nm range with a Sellmeier model [10]. With a deposition temperature much larger than here and unspecified between 673 and 973 K, Dujardin et al. [30] plotted the absorption coefficient in the 122-270-nm range of CeF_3 films deposited by molecular beam epitaxy. Other than experimental data for films, Saini [31] theoretically calculated the refractive index of crystalline CeF_3 in the 0-30-eV range.

The reported literature lacks self-consistent optical–constant data for these materials, which may result in an inaccurate computation of the optical properties of multilayer coatings with these fluorides. This research is devoted to obtain self-consistent optical constants of thin films of the three fluorides deposited by evaporation onto substrates at 523 K in a broad spectral range. This paper is organized as follows. Section 2 describes sample preparation of thin films deposited by boat evaporation and measurement techniques. Section 3 presents the procedure used to calculate optical constants, which involves the use of two successive Kramers-Kronig (KK) analyses. Section 4 presents optical measurements on thin films of MgF_2, LaF_3, and CeF_3 through a combination of reflectance, transmittance, and ellipsometry measurements covering the spectral range from 30 to 950 nm. These measurements were extended to a much larger spectral range with literature data and extrapolations to perform the KK analyses, from which the optical constants were obtained. The self-consistency of the obtained optical constant sets is evaluated both with well-known sum rules that provide the global consistency evaluation [32] as well as with recent sum rules developed to evaluate consistency at the desired spectral range [33].

2. Experimental techniques

Thin films of MgF_2, LaF_3, and CeF_3 were prepared by evaporation from tungsten boats. Evaporation materials of 99.99% purity (LaF_3 and CeF_3) and VUV-grade (MgF_2) were used. Deposition was performed in a 50-cm side cube chamber pumped with a turbomolecular system and a liquid-N_2 cooled, Ti sublimation pump. The distance between evaporation source and substrate was 30 cm.

Base pressure was ~1.5 × 10^{-5} Pa; pressure increased during deposition up to 4 × 10^{-5} Pa (MgF$_2$ and LaF$_3$) or 6 × 10^{-4} Pa (CeF$_3$). Average deposition rate was 0.3 nm/s. Substrate temperature was set at 523 K. A set of three samples were prepared in each run: one on a BK-7 glass substrate for FUV-extreme UV (EUV), and x-ray reflectance measurements (MgF$_2$ and CeF$_3$), one on a MgF$_2$ crystal substrate for transmittance measurements, and one on a piece of a Si wafer for ellipsometry measurements and, only for LaF$_3$, also for reflectance and x-ray reflectance measurements. After deposition, samples were let to cool down at a rate not faster than 1 K/min. Film thickness was monitored with a quartz crystal; film thickness was measured a posteriori through stylus profilometry (except for LaF$_3$), and from the fit to both grazing-incidence x-ray reflectometry and ellipsometry measurements. The available measurements are displayed in Table 1 and the average of these measurements was taken as the final thickness: 44, 48, and 40 nm for the sets of samples of MgF$_2$, LaF$_3$, and CeF$_3$, respectively.

Table 1. Film thicknesses in nm obtained through different techniques

Material	Profilometry	Ellipsometry	x-ray reflectometry	Average
MgF$_2$	43	44	46	44
LaF$_3$	-	48	48	48
CeF$_3$	39	40	40	40

Sample reflectance and transmittance were measured in GOLD's (acronym for Grupo de Optica de Láminas Delgadas) reflectometer system in the 30-190 nm range. The reflectometer has a grazing-incidence, toroidal-grating monochromator, in which the entrance and exit arms are 146° apart. The monochromator covers the 12.5-200 nm spectral range with two Pt-coated diffraction gratings that operate in the long (250 l/mm) or in the short (950 l/mm) spectral range. A windowless capillary discharge lamp was used in this work. The lamp is fed with various pure gases or gas mixtures with which it can generate many spectral lines to cover the spectral range of interest. The beam divergence was ~1.7 mrad. The sample holder can fit samples up to an area of 50.8x50.8 mm^2. A channel electron multiplier with a CsI-coated photocathode was used as the detector. Reflectance and transmittance were obtained by alternately measuring the incident intensity and the intensity reflected or transmitted, respectively, by the sample. Transmittance was measured at normal incidence and reflectance was measured at 5° away from the normal. FUV-EUV reflectance and transmittance uncertainty are estimated to be ~ ± 2%.

In the near UV and longwards, Perkin-Elmer Lambda-9 and Lambda-900 double-beam spectrophotometers were used to measure regular transmittance and specular reflectance with the universal reflectance accessory, respectively, in the 190-2000-nm range. For reflectance and transmittance measurements, samples were situated at 8° and 1.5° from normal incidence, respectively.

Ellipsometry measurements were performed with a GES-5E Sopralab Spectroscopic Ellipsometer. The incidence angle at which measurements were performed was optimized around Si Brewster angle at the Si bandgap by confining the spectral distribution of cosΔ symmetrically around zero in order to maximize accuracy.

Grazing incidence x-ray reflectometry measurements were performed at Centro de Asistencia a la Investigación, Universidad Complutense de Madrid. The diffractometer was a PANalytical X`pert PRO MRD. The source was a Cu anode under 45 kV discharge. The Cu Kα (λ = 0.154 nm) line was selected by means of a graphite monochromator. Measurements were performed at the grazing incidence angles from 0.15° to 2.5°, with a step of 0.005°. x-ray reflectometry was used to evaluate film thickness, surface roughness, and density. To fit these parameters, the optical constants of the materials were downloaded from CXRO's web [34] and reflectance versus incidence angle were calculated and compared with measurements. At these short wavelengths, k and δ = 1-n can be considered proportional to

density. Film density, thickness, and roughness were let to vary until the best match was obtained.

3. Optical constants calculation procedure

The optical constants of MgF_2, LaF_3, and CeF_3 films were calculated through an iterative double KK analysis. The present procedure reproduces the scheme followed in a research performed to obtain the optical constants of SiO_2 and Ta_2O_5 films [35]. The process was iterated twice for each material until a self-consistent set $\{n,k\}$ was obtained that best fitted all ellipsometry and photometry measurements. One of the KK analyses was performed in reflectance and the other one in the extinction coefficient k:

$$\phi(E) = -\frac{E}{\pi} P \int_0^\infty \frac{\ln\left[R(E')\right]}{E'^2 - E^2} dE' \tag{1}$$

$$n(E) - 1 = \frac{2}{\pi} P \int_0^\infty \frac{E'k(E')}{E'^2 - E^2} dE' \tag{2}$$

where P stands for the Cauchy principal value. Equations (1) and (2) relate reflectance with its phase, and k with the real part of the refractive index n, respectively. Complex reflectance is given by r = $R^{1/2}$exp(iϕ), where $R^{1/2}$ and ϕ stand for its modulus and phase, respectively. Integration is performed over photon energy E. Each KK analysis requires data over the whole spectrum, for which experimental data are completed with extrapolations.

The need to use the two sorts of KK analyses arises in the initial lack of data for both of them. Hence, to perform the integration in reflectance (odd iterations), available measurements in part of the FUV range were affected by the contribution to reflectance of the film-substrate interface (due to the transparency of the fluoride film), which does not let us obtain n and k from R and ϕ. Regarding integration in the extinction coefficient (even iterations), k data in the EUV range was not available due to the lack of transparent massive substrates. Each iteration of the present procedure obtains the necessary data to fill in the next iteration. Four iterative KK analyses resulted in self-consistent data sets which reasonably fitted the experimental photometric and ellipsometry measurements.

Experimental data included transmittance, reflectance, and ellipsometry measurements; the covered range was extended with extrapolations. In the following the data sources used to perform KK integrations are specified; moreover, data sources and the iterative procedure are summarized in Table 2:

i) Between 0.041 nm ($3 \cdot 10^4$ eV) and 30 nm, Henke's semiempirical data were used, which were downloaded from the Web site of Center for X-Ray Optics (CXRO) at Lawrence Berkeley National Laboratory [34]). k data was used in k integration and n and k were used to calculate the reflectance of an opaque film in reflectance (R) integration. k was further extended to larger energies with a power function. The densities of the materials, which are required to complete these data, were measured and are presented in subsection 4.4.

ii) Between 30 nm and ~114 nm, there was no experimental k data due to the lack of transparent massive substrates in most of the range. In this spectral range reflectance was measured, and hence the first iteration was an R-ϕ KK analysis. Out of the R-ϕ data at near-normal incidence, n and k can be obtained using the well-known reflectance formula of a single interface:

$$r = \frac{(n + ik) - 1}{(n + ik) + 1} \tag{3}$$

where r=$R^{1/2}$exp(iφ). For this formula to apply, the fluoride layer must be opaque, which is satisfied in this range. Eq. (3) is inverted to obtain the optical constants:

$$n + ik = \frac{1+r}{1-r} \qquad (4)$$

Eq. (4) is a complex equation and hence both n and k can be calculated. k data obtained through Eq. (4) are used in the even iterations.

iii) Between ~114 and 190 nm, k was calculated out of transmittance measurements. For the first KK analysis in k (iteration 2), k was calculated with the well-known Beer-Lambert law:

$$\frac{T_{fs}}{T_s} = \exp\left(-\frac{4\pi k z}{\lambda}\right) \qquad (5)$$

where T_s and T_{fs} are the transmittance of the uncoated MgF_2 substrate and of the substrate coated with the film, respectively; z and λ represent film thickness and wavelength. Light reflected both at the outer as well as at the inner interfaces is neglected in Eq. (5). After a preliminary set of optical constants was available, exact transmittance, including internal interferences and reflectance, could be calculated in iteration 3 [hence Eq. (5) was not used in this iteration].

Regarding reflectance, experimental values were used in the first R-ϕ KK analysis, whereas calculated reflectance (from optical constants obtained from iteration 2) was used in the second R-ϕ KK analysis. Calculated reflectance of an opaque film was used instead of experimental reflectance because the latter was affected by interferences with the substrate, as fluorides turn transparent in this spectral range. As a reminder, to obtain n and k from reflectance using Eq. (4), the contribution from the inner interfaces must be negligible.

iv) Between 190 and 950 nm, ellipsometry measurements were fitted with one (MgF_2 and LaF_3) or five (CeF_3) Lorentz oscillators. k or reflectance were calculated with the single or multiple Lorentz oscillators obtained in the fit and were used in all iterations.

v) Above 950 nm, the Lorentz oscillator(s) fitted in the 190-950-nm range were extrapolated, which were used to calculate k or reflectance for the three materials.

The sequence of R-ϕ and n-k KK integrals through four successive iterations is explained in the following. An initial $\{R_1\}$ set was used for a first R-ϕ KK integration, from which an initial $\{n_1,k_1\}$ set was obtained using Eq. (4). Then, for the first n-k KK integration, a $\{k_2\}$ data set was gathered, from which a second $\{n_2,k_2\}$ set was obtained. Next, a new $\{R_2\}$ set was gathered for a second R-ϕ KK integration, from which a third $\{n_3,k_3\}$ set was obtained. Finally, $\{k_4\}$ data set was gathered and used in a second n-k KK integration, from which a fourth and final $\{n_{final}, k_{final}\}$ set was obtained. $\{k_2\}$ and $\{k_{final}\}$ data sets included parts of $\{k_1\}$ and $\{k_3\}$ data obtained in the previous iteration, respectively, as displayed in Table 2. $\{R_2\}$ included parts of calculated reflectance with $\{n_2,k_2\}$. The procedures and their data sources are summarized in Table 2.

The optical properties of fluoride films may somewhat depend on film thickness. When fluoride films become thicker, their packing density often reduces, which must result in some kind of a gradient in the optical constants. Film density of the present fluorides stand at ~95% of the bulk density (see Sub-section 4), which can be considered rather high if we compare it with the low packing density of fluoride films when deposited at room temperature. The thickness at which such gradient must be significant will depend on substrate temperature. For MgF_2 films deposited by evaporation, Kolbe et al. [13] measured a packing density not far from 100% for a 300-nm thick film deposited at a temperature close to 523 K, so that no significant gradient is expected up to such a film thickness. For LaF_3 films, the same research did not measure density but calculated the refractive index and absorption coefficient and found a gradient for 300-nm thick films. Thielsch et al. [24] found that LaF_3 films deposited at 523 K grew with some gradient; they developed a model in which the inner 40-nm thick

sublayer was considered homogeneous. The present LaF_3 film thickness is only slightly above that limit. Bischoff et al. [36] measured the packing density of LaF_3 films deposited at 423 K and found it to be within ~90%-100% of the bulk value for films up to 50 nm; the limiting thickness for high packing density can be expected to be larger for films deposited at 523 K than at 423 K. According to the above, the present 48-nm thick LaF_3 film can be considered mostly homogeneous, although packing density is expected to decrease with larger thickness. We found no data on homogeneity for CeF_3 films, but its relatively high packing density suggests that the present film is mostly homogeneous. Summarizing, the present films for the three fluorides can be considered homogeneous in depth, but the use of the below optical constants on thicker films, at least for LaF_3, may require some gradient model of the layer and new optical measurements to characterize that gradient.

Table 2. Scheme of the data sources for the iterative KK analysis[a].

Iteration	Spectral range					Produced optical constants
	$\lambda<30$ nm	30-114 nm	114-190 nm	190-950 nm	$\lambda>950$ nm	
1. R-ϕ KK. $\{R_1\}$	R CXRO	R experimental		R from Lorentz oscillator(s) fitted from E	R from Lorentz oscillator(s) extrapolation	$\{n_1, k_1\}$
2. k-n KK. $\{k_2\}$	k CXRO	k from iteration 1	k from transmittance, neglecting R MgF_2: T noisy $\rightarrow$ smooth connection at 180-190 nm	k from Lorentz oscillator(s) fitted from E	k from Lorentz oscillator(s) extrapolation	$\{n_2, k_2\}$
3. R-ϕ KK. $\{R_2\}$	R CXRO	R experimental	R calculated from iteration 2 with $\{n_2, k_2\}$	R from Lorentz oscillator(s) fitted from E	R from Lorentz oscillator(s) extrapolation	$\{n_3, k_3\}$
4. k-n KK. $\{k_{final}\}$	k CXRO	k from iteration 3	k from transmittance. Exact calculations including R and interferences MgF_2: T noisy $\rightarrow$ smooth connection at 180-190 nm	k from Lorentz oscillator(s) fitted from E	k from Lorentz oscillator(s) extrapolation	$\{n_{final}, k_{final}\}$

[a]: R: reflectance. T: transmittance. E: ellipsometry

Other parameters, such as substrate material and deposition rate, might also somewhat influence the optical constants. The influence of substrate material was not investigated here because the procedure used to obtain the optical constants relies on measurements with various techniques over the spectrum that were performed on samples prepared with different sorts of substrates. Regarding deposition rate, all samples prepared to measure with the different techniques (reflectance, transmittance, ellipsometry) were deposited in the same run and hence their deposition rate was the same; no further effort was performed to repeat the characterization process for samples deposited at different rates.

Even though the three fluorides analyzed here are uniaxial crystals when bulk and hence are birefringent, thin films of these materials deposited at a temperature far below the material melting point are expected to grow in the form of nanocrystals with random orientations, which results in films with no effective birefringence.

4. Experimental results

4.1. Optical constants of MgF_2

Figure 1(a) displays the transmittance of the MgF_2 film normalized to the transmittance of the bare MgF_2 substrate; half of the MgF_2 substrate was left uncoated for this purpose. Transmittance in the near UV and at longer wavelengths was indistinguishable from the

transmittance of the bare substrate. Even in the long FUV, absorption in the film was very small so that the transmittance ratio, i.e., normalized to substrate transmittance, was not far from unity and hence transmittance looks somewhat noisy. Figure 1(b) displays the reflectance of the MgF_2 film deposited on a glass substrate. Figure 2 displays the ellipsometry measurements at 78° on the MgF_2 film deposited on a Si wafer, and the fit performed with a single Lorentz oscillator. The oscillator was used in the iterative process described in section 3 to calculate the optical constants in the 190-950-nm spectral range and also at longer wavelengths. The Lorentz oscillator parameters of MgF_2 and also of LaF_3 and CeF_3 are given in Table 3. Silicon wafer substrates were previously characterized: ellipsometry measurements were performed on a part of the wafer where no coating was deposited, from which the thickness of the native SiO_2 was obtained; optical constants of Si [37] and SiO_2 [38] were used for modelling the Si wafer and its native oxide.
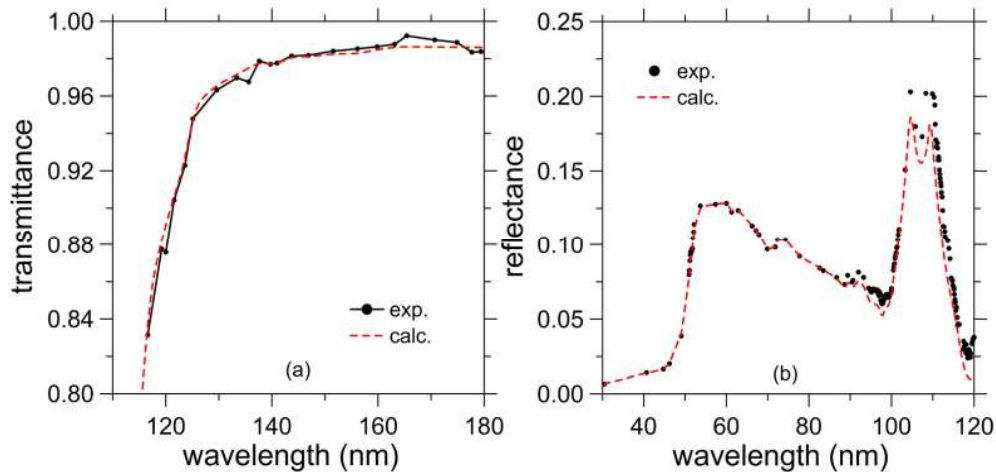
Fig. 1. Comparison between the experimental measurements and calculations with MgF_2 optical constants obtained in this subsection. a: transmittance (normalized to the transmittance of the bare MgF_2 substrate) of a 44-nm thick film. b: reflectance of a 44-nm thick MgF_2 film on a glass substrate

The final self-consistent set of optical constants, referred to as $\{n_{final}, k_{final}\}$, obtained after iteration 4, is displayed in Fig. 3. With the final optical constants, normalized transmittance, reflectance, and ellipsometry parameters were calculated and are also plotted in Figs. 1 and 2. There is a satisfactory match between calculation and experimental values.
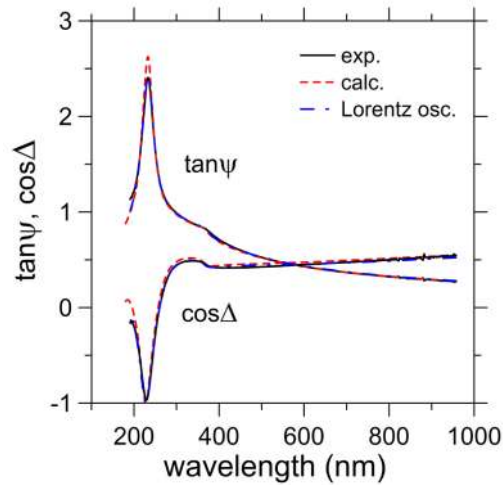
Fig. 2. Ellipsometry measurements at 78° on a 44-nm thick MgF$_2$ film deposited on a Si wafer, along with the fit performed with a single Lorentz oscillator and calculations with optical constants obtained in this subsection
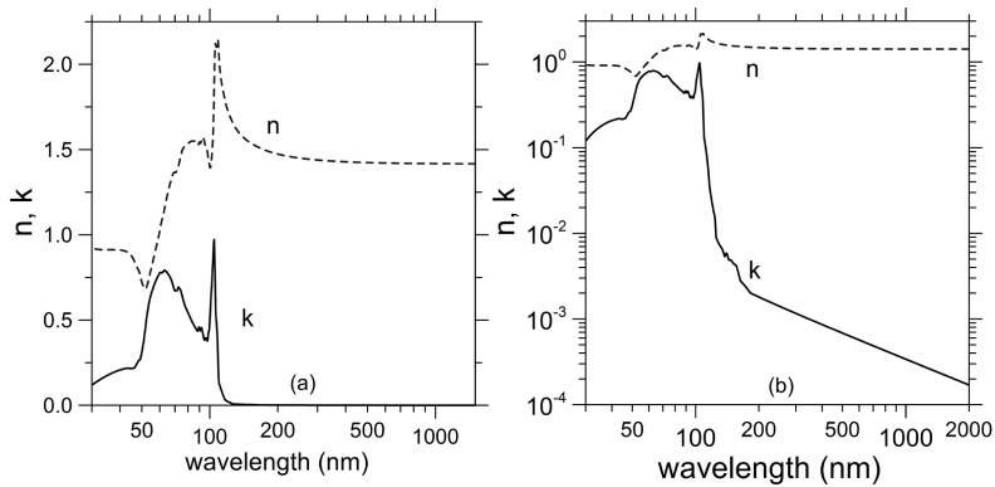

Fig. 3. Optical constants of MgF$_2$ films deposited at 523 K (a: linear-axis; b: log-axis) versus wavelength in log scale.

4.2. Optical constants of LaF$_3$

Figure 4(a) displays the transmittance of the LaF$_3$ film normalized to the transmittance of the bare MgF$_2$ substrate. Figure 4(b) displays the reflectance of the LaF$_3$ film deposited on the Si wafer. Figure 5 displays the ellipsometry measurements at 74° on the LaF$_3$ film deposited on Si wafer, and the fit performed with a single Lorentz oscillator, which precisely reproduces the experimental data. The Si wafer was previously characterized as described in sub-section 4.1. The final self-consistent set of optical constants, referred to as {n_{final}, k_{final}} obtained after iteration 4 is displayed in Fig. 6.

Table 3. Parameters of the fits to ellipsometry data with Lorentz oscillators[a] defined as
$$-A\lambda^2\big/\left(\lambda_0^2 - \lambda^2 + i\gamma\lambda\right)$$

Material	λ_0 (nm)	γ (nm)	A
MgF$_2$	80.5	1.87	1.73
LaF$_3$	69.1	0.49	2.55
CeF$_3$, LO1	73.7	2.69	2.39
CeF$_3$, LO2	205.7	4.49	0.00081
CeF$_3$, LO3	216.6	8.08	0.0060
CeF$_3$, LO4	231.7	8.55	0.0061
CeF$_3$, LO5	246.8	14.10	0.020

[a]: CeF$_3$ was fitted to the addition of 5 Lorentz oscillators
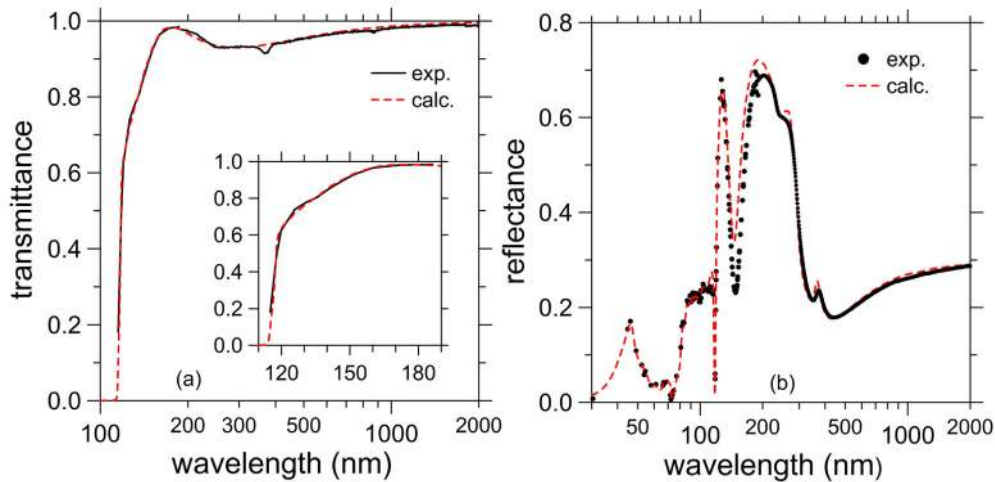
Fig. 4. Comparison between the experimental measurements and calculations with LaF$_3$ optical constants obtained in this subsection. a: transmittance (normalized to the transmittance of the bare MgF$_2$ substrate) of a 48-nm thick film; the inset highlights the 110-190 nm range. b: reflectance of a 48-nm thick film on a Si substrate. Wavelength is in log scale

With the final optical constants, normalized transmittance, reflectance, and ellipsometry parameters were calculated and are also plotted in Figs. 4 and 5, respectively. For reflectance calculations in the transparency range of LaF$_3$, the Si wafer substrate was modelled with the optical constants mentioned above for ellipsometry fittings.

A small dip in experimental transmittance data was found at around ~360 nm, which was attributed to an artifact of the spectrophotometer, since the instrument changes a filter at that wavelength. Other than that feature, there is a good overall match between calculation and experimental values.

4.3. Optical constants of CeF$_3$

Figure 7(a) displays the transmittance of the CeF$_3$ film normalized to the transmittance of the bare MgF$_2$ substrate. Figure 7(b) displays the reflectance of the film deposited on a glass substrate. CeF$_3$ presents weak absorption peaks at various wavelengths (211 nm, 216 nm, 231 nm, and 246 nm) longer than the cutoff at ~120 nm. Similar weak absorption peaks have been reported in the literature [25, 30, 39], which were attributed to the 4f→5d transitions of Ce^{3+} ions. Figure 8 displays the ellipsometry measurements at 72° on the film deposited on the Si

wafer and the fit performed with five Lorentz oscillators. The Si wafer was previously characterized as described above. For this material, a single oscillator did not provide a good fit of the experimental data because of the multi-peak absorption observed in the ~190-250 nm spectral range; the number of Lorentz oscillators in the fit was increased to five to reproduce this absorption. Four out of the five oscillators are included to fit the four small-absorption peaks that can be seen in the transmittance figure. The other oscillator plays the same role that the single oscillator for MgF_2 and LaF_3: it provides the tail of decreasing k with increasing wavelength due to the strong absorption below the material cutoff. The final self-consistent set of optical constants, referred to as $\{n_{final}, k_{final}\}$, obtained after iteration 4, is displayed in Fig. 9.
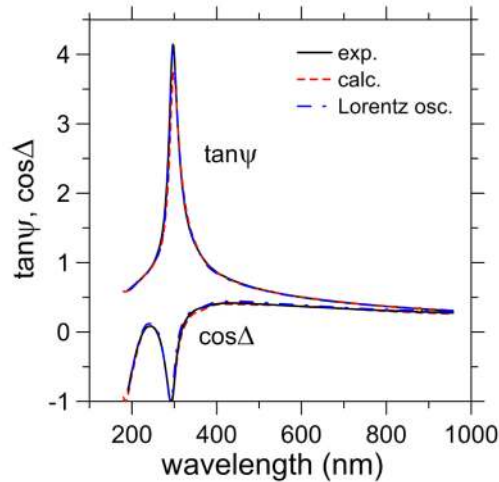
Fig. 5. Ellipsometry measurements at 74° on a 48-nm thick LaF_3 film deposited on a Si wafer, along with the fit performed with a single Lorentz oscillator and calculations with optical constants obtained in this subsection
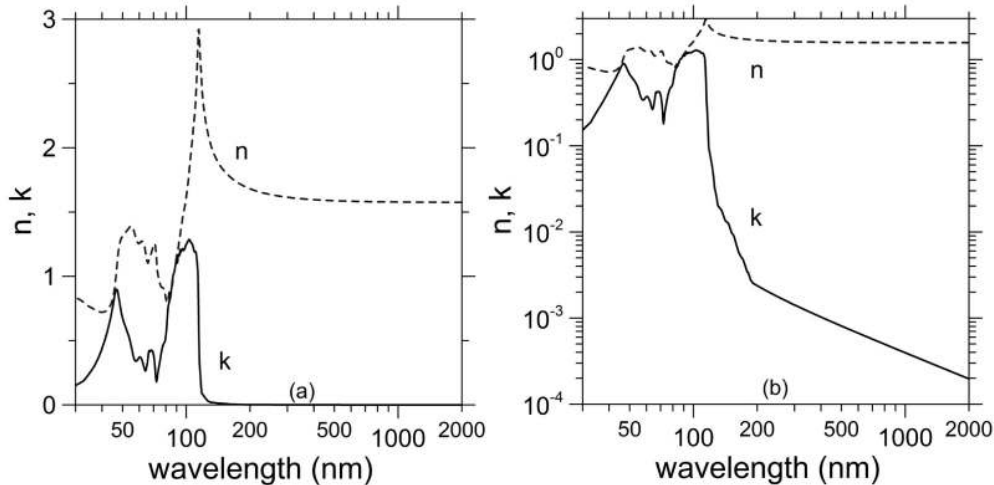
Fig. 6. Optical constants of LaF_3 films deposited at 523 K (a: linear axis; b: log-axis) versus wavelength in log scale.

With the final optical constants, normalized transmittance, reflectance, and ellipsometry parameters were calculated and are also plotted in Figs. 7 and 8, respectively. There is an excellent match between calculation and experimental values. As with LaF_3, a small dip was

found in experimental transmittance data at around ~360 nm, which was again attributed to a filter change in the spectrophotometer.
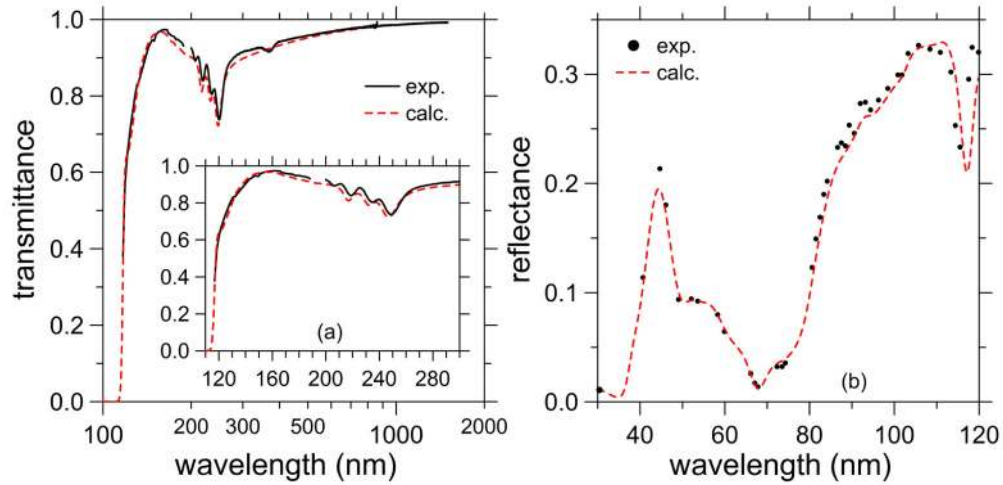

Fig. 7. Comparison between the experimental measurements and calculations with CeF$_3$ optical constants obtained in this subsection. a: transmittance (normalized to the transmittance of the bare MgF$_2$ substrate) of a 40-nm thick film vs. wavelength in log scale; the inset highlights the 110-300 nm range. b: reflectance of a 40-nm thick film on a glass substrate.
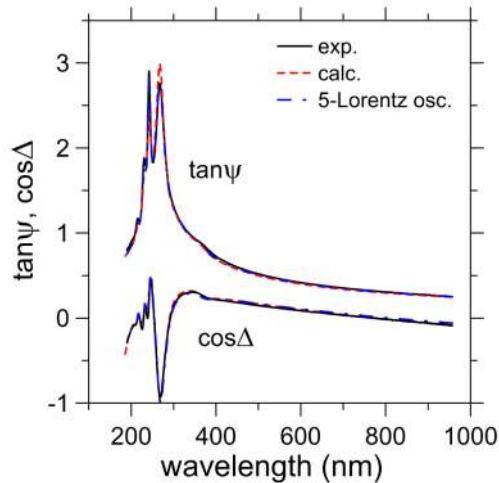

Fig. 8. Ellipsometry measurements at 72° on a 40-nm thick CeF$_3$ film deposited on a Si wafer, along with the fit performed with 5 Lorentz oscillators and calculations with the optical constants obtained in this subsection.

4.4. Optical constant consistency

The consistency of the optical constants was evaluated with sum rules, named as *f*- and inertial sum rules. Conventional sum rules applied to a set of optical constants provides a global evaluation of their consistency, but give no information of the possible lack of consistency at a specific spectral range. Novel sum rules have been recently proposed [33] that enable obtain information of optical-constant consistency at the desired spectral range. The consistency of the present optical constant sets of fluoride films are checked below both globally and locally. *f*-sum rule is expressed by:

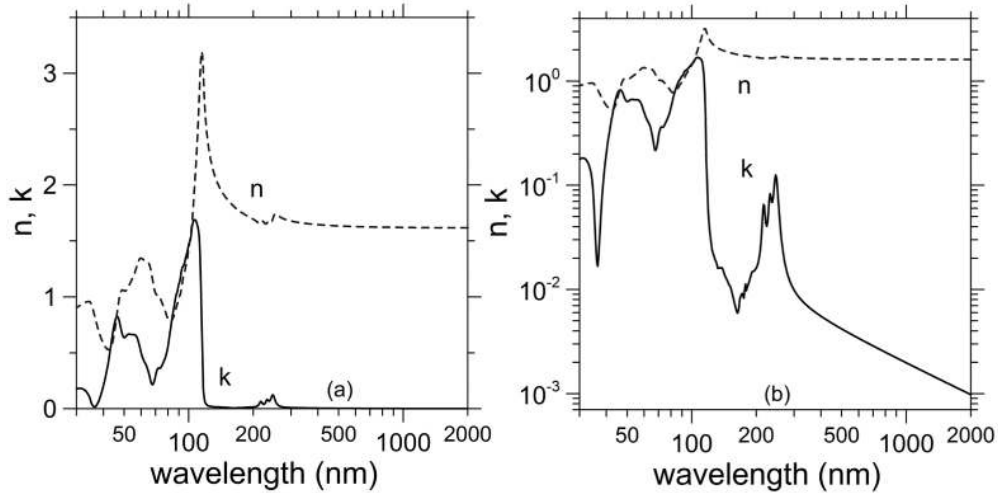$$n_{eff} = \frac{4\varepsilon_0 m}{\pi N e^2 \hbar^2} \int_0^\infty E' k(E') dE' \tag{6}$$

Fig. 9. Optical constants of CeF_3 films deposited at 523 K (a: linear axis; b: log-axis) versus wavelength in log scale.

where e and m are the electron charge and mass, respectively, ε_0 is the permittivity of vacuum, $\hbar$ is the reduced Planck's constant, and N is the electron density. n_{eff} represents the total number of electrons in the molecule, which should be 30, 84, and 85, for MgF_2, LaF_3 and CeF_3, respectively. When the relativistic correction on scattering factors is taken into account, n_{eff} is somewhat modified: the theoretical effective number of electrons is reduced to 29.98 (MgF_2), 83.53 (LaF_3) and 84.51 (CeF_3) [40]. The density of MgF_2, LaF_3, and CeF_3 film samples was measured through grazing incidence x-ray reflectance measurements at Cu K_α line ($\lambda = 0.154$ nm), which were fitted with IMD software [41]. Density values of 2.99 g/cm^3, 5.79 g/cm^3, and 5.87 g/cm^3 were obtained for MgF_2, LaF_3 and CeF_3, which are 94.6%, 97.5%, and 95.3% of their bulk density, respectively. The integral of Eq. (6) with the present k data results in 30.62, 83.01, and 86.21 for MgF_2, LaF_3 and CeF_3, respectively. The deviations are 2.1%, −0.6% and 2.0% for MgF_2, LaF_3 and CeF_3, respectively, which can be considered acceptable numbers.

The other global consistency check is obtained with the inertial sum rule:

$$\int_0^\infty [n(E) - 1] dE = 0 \tag{7}$$

which is evaluated with the following normalization [42]:

$$\zeta = \frac{\int_0^\infty [n(E) - 1] dE}{\int_0^\infty |n(E) - 1| dE} \tag{8}$$

A satisfactory range for ζ is usually established within ± 0.005 [43]. Values of $\zeta = 1.8 \times 10^{-5}$, -4.8×10^{-5}, and -0.7×10^{-5} were obtained for MgF_2, LaF_3 and CeF_3, respectively, well within the above limit.

Let us now evaluate the local consistency of the obtained optical constants [33]. The method that is applied enables enhancing the weight of a desired spectral range within the

sum-rule integral. The procedure consists in multiplying the complex refractive index with a complex window function constructed to have more weight at the desired spectral range. The window functions proposed in Ref [33] were used:

$$H_1(E) = \frac{1}{\pi}\left[L(E;E_2,c) - L(E;E_1,c)\right] \tag{9}$$

and

$$H_2(E) = \frac{1}{\pi}\left[L(E;E_2,c_2) + L(E;E_1,c_1) - 2L\left(E;\sqrt{E_1E_2},\frac{c_1+c_2}{2}\right)\right] \tag{10}$$

with:

$$L\left(E;E_j,c\right) \equiv \ln\left(E_j^2 - E^2 - icE\right) \quad j=1,2 \tag{11}$$

where ln stands for natural logarithm, which is understood as the logarithm principal value, i.e., its imaginary part lies in the interval $(-\pi,\pi]$. $[E_1,E_2]$ is the photon-energy spectral range where the above window functions take larger values, in order to increase the relative weight of the optical constants in this spectral range in the sum-rule integration. The shape of H_1 and H_2 can be seen in Ref [33].

The following sum rules were used here [33]:

$$\int_0^\infty E'^{-2} \,\mathrm{Re}\{H_2(E')[N(E')-1]\}\,dE' = 0 \tag{12}$$

$$\int_0^\infty E'^{-1} \,\mathrm{Im}\{H_2(E')[N(E')-1]\}\,dE' = 0 \tag{13}$$

$$\int_0^\infty \mathrm{Re}\{H_2(E')[N(E')-1]\}\,dE' = 0 \tag{14}$$

$$\int_0^\infty E'\,\mathrm{Im}\{H_2(E')[N(E')-1]\}\,dE' = 0 \tag{15}$$

$$\int_0^\infty E'^2 \,\mathrm{Re}\{H_2(E')[N(E')-1]\}\,dE' = 0 \tag{16}$$

$$n_{eff} = \frac{4m\varepsilon_0}{\hbar^2 Ne^2\left(E_1^2 - E_2^2\right)}\int_0^\infty E'^3 \,\mathrm{Im}\{H_1(E')[N(E')-1]\}\,dE' \tag{17}$$

The last sum rule resembles f-sum rule and the other five sum rules show similarities with the inertial sum rule. In spite of the resemblance, the novel sum rules involve a larger contribution to the integral of a desired spectral range, which is achieved through the election of E_1 and E_2.

In order to obtain the consistency at each spectral range, the window function is made to continuously scan the spectrum. Hence the window function is centred at a variable energy E_w, which is scanned over the spectrum. In the below calculations, E_w and the window limits E_1 and E_2 were set at $E_w = (E_1E_2)^{0.5}$ (E_w is the geometric average of E_1 and E_2) and $E_2/E_1 = 3$.

Figure 10 plots ζ vs E_w for the above sets of optical constants of MgF_2, LaF_3 and CeF_3, respectively, using the five sorts of inertial-like sum-rules (Eq. (12) to Eq. (16)) with window

function H_2 and window parameters $c_{1(2)} = E_{1(2)}/10$. A straightforward generalization of the evaluation parameter given by Eq. (8) has been used [33]. Each point in Fig. 10 represents ζ calculated with one of the above sum rules where the window function has been centred at the corresponding energy E_w. Parameter ζ comfortably stands within the ± 0.005 limit in almost all the plotted spectral range investigated for all sum rules and materials. This indicates that the optical constants are locally consistent at each photon energy range in this wide spectrum. There is a trend to diverge at energies larger than the plotted ones, which starts at smaller energies for sum rules with a larger energy power in the integrand.
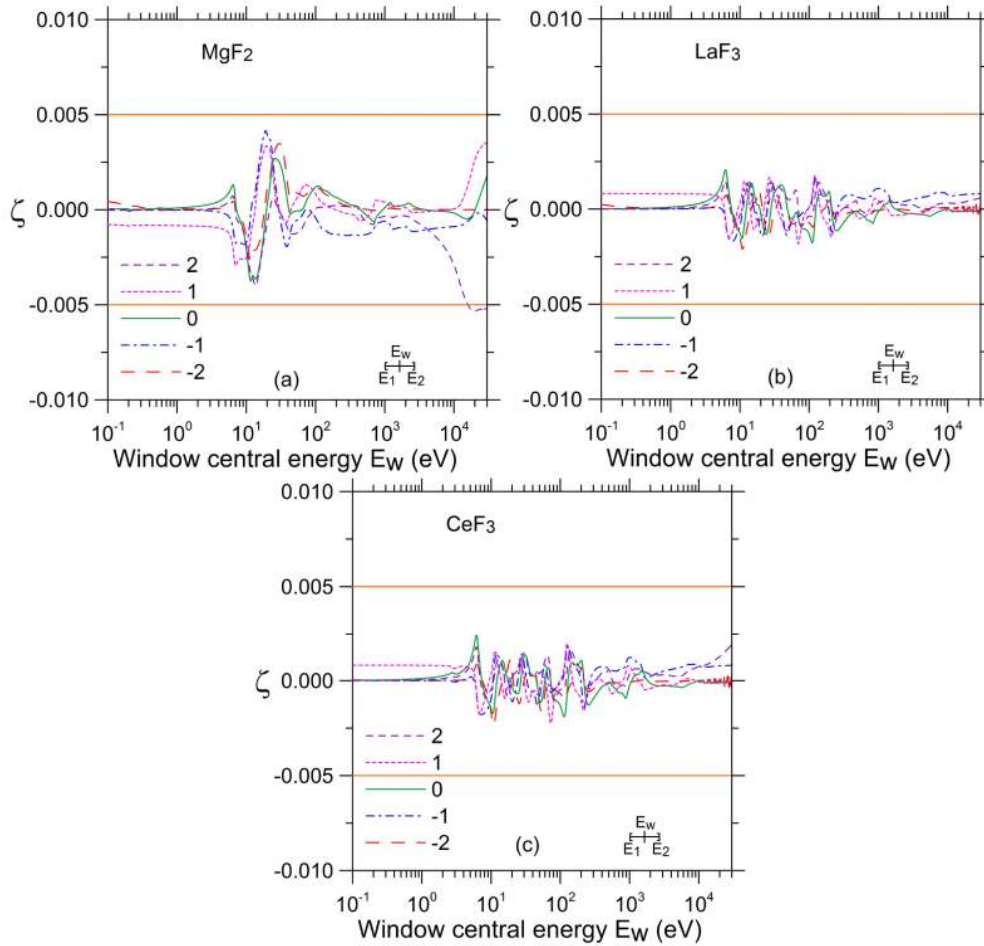

Fig. 10. The evaluation parameter ζ versus the central energy E_w for sum rules represented through Eqs. (12) to (16) calculated with H_2 window function and with the optical constants of MgF_2 (a), LaF_3 (b), and CeF_3 (c). The five inertial-like sum rules are identified in the legend with the power of photon energy in the integral. Window function parameters at each E_w are given by: $E_w = (E_1E_2)^{0.5}$, $E_2/E_1 = 3$, and $c_{1(2)} = E_{1(2)}/10$. The suggested acceptable limits at $\pm$ 0.005 are also plotted

Figure 11 plots n_{eff} for the sum rule given by Eq. (17) with H_1 window function applied to the optical constants of the three fluorides with the same value of E_w and with $c = E_1/5$. The sum of electrons in the molecules, once corrected for relativistic effects, was mentioned to be 29.98 (MgF_2), 83.53 (LaF_3) and 84.51 (CeF_3); Fig. 11 shows that the deviation from these numbers over the plotted spectral range reaches a maximum of 2.1% and −0.6% for MgF_2 and LaF_3, respectively, which equal what was obtained with the application of the global f-sum rule; the deviation stands between 2.0% and 2.3% for CeF_3, the top value only slightly larger

than for the global sum rule. These numbers suggest that the optical constants are consistent at each part of the spectrum. The curves start diverging at large energies, what was also observed with the inertial-like sum rules. Sum rule given by Eq. (17) is strongly biased towards high energies due to the E^3 term within the integrand, which may be the reason why n_{eff} starts diverging in this sum rule at a smaller energy than for the inertial-like sum rules. This feature has not been investigated in depth but it suggests that experimental values of the optical constants might be required at larger energies. Nevertheless, since the conjectural lack of self-consistency obtained is found far away from the spectral range covered in this research, it seems not to be a challenge for the consistency of the optical constants in the present range.
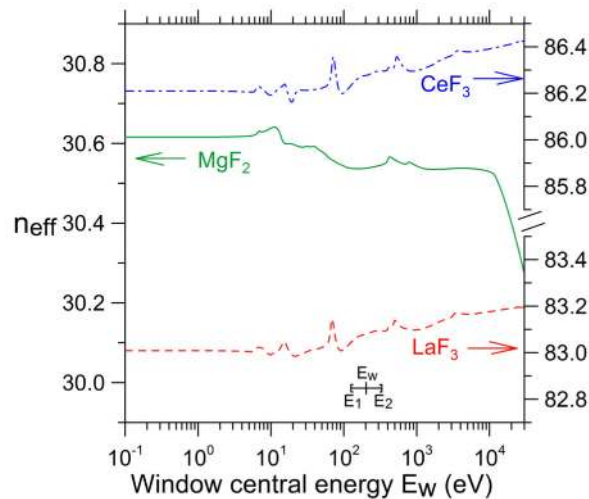

Fig. 11. n_{eff} versus the central energy E_w for sum rule represented through Eq. (17) calculated with H_1 window function and with the optical constants of MgF_2, LaF_3, and CeF_3. Window function parameters at each E_w are given by: $E_w = (E_1 E_2)^{0.5}$, $E_2/E_1 = 3$, and $c = E_1/5$

Summarizing, both classical f- and inertial-sum rules, along with new sum rules involving window functions, resulted in satisfactory evaluation parameters, which suggests a good consistency of the sets of optical constants obtained for MgF_2, LaF_3 and CeF_3 films. The optical constants here presented are available upon request at the following e-mail address: j.larruquert@csic.es.

Conclusions

Self-consistent optical constants of thin films of MgF_2, LaF_3, and CeF_3 deposited by evaporation onto substrates at 523 K have been determined in the spectral range of 30-950 nm. The optical constants obtained for the three fluorides can be useful for the design of interference optical coatings. The optical constants were obtained from a combination of transmittance (FUV range), reflectance (EUV and FUV ranges), and ellipsometry measurements (from the near UV to the near IR ranges), along with extrapolations, from which data sets of k and reflectance were gathered over the whole spectrum. A consistent set of optical constants for each fluoride was obtained using KK analyses relating both reflectance with its phase and k with n; the KK analyses were applied iteratively until the obtained sets of optical constants were successful to satisfactorily reproduce all experimental measurements.

The consistency of the optical constants of the three fluoride films was evaluated with the use of sum rules. The global consistency of optical-constant data over the whole spectrum was found to be satisfactory through the use of standard f- and inertial sum rules. Furthermore, the local consistency of the optical-constant data sets at each photon energy

range was also found satisfactory through the use of sum rules with window functions. To the best of our knowledge, these are the first self-consistent sets of optical constants of MgF_2, LaF_3, and CeF_3 thin films deposited onto substrates heated at a temperature close to 523K that involve experimental data from the EUV to the NIR. For CeF_3 films, no FUV data were found for films deposited at a close temperature (no n data in the FUV at all), so that the present set provides a broad range of new and self-consistent data.

Funding

Acknowledgments